Modified Pulse Repetition Coding Boosting Energy Detector Performance in Low Data Rate Systems

Florian Troesch, Frank Althaus, and Armin Wittneben
Swiss Federal Institute of Technology (ETH) Zurich
Communication Technology Laboratory, CH-8092 Zurich, Switzerland
Email: troesch@nari.ee.ethz.ch

***Abstract*— We consider *Ultra-Wideband Impulse Radio* (UWB-IR) *Low Data Rate* (LDR) applications where a more complex *Cluster Head* (CH) communicates with many basic *Sensors Nodes* (SN). At receiver side, noncoherent *Energy Detectors* (ED) operating at low sampling clock, i.e., below $300\,\mathrm{kHz}$, are focused. Drawback is that EDs suffer from significant performance losses with respect to coherent receivers. *Pulse Repetition Coding* (PRC) is a known solution to increase receiver performance at the expense of more transmit power. But in LDR systems known PRC is very inefficient due to the low receiver sampling clock. Boosting transmit power is not possible due to *Federal Communications Commission's* (FCC) power constraints. Hence, we present a modified PRC scheme solving this problem. *Modified Repetition Coded Binary Pulse Position Modulation* (MPRC-BPPM) fully exploits FCC power constraints and for EDs of fixed integration duration is optimal with respect to *Bit Error Rate* (BER). Furthermore, MPRC-BPPM combined with ED outperforms SRAKE receivers at the expense of more transmit power and makes ED's performance robust against strong channel delay spread variations.**

I. Introduction

Recently, *Ultra-Wideband Impulse Radio* (UWB-IR) technology has gained strong interest as a very promising technology for future indoor wireless communication. Key applications for which UWB-IR technology is considered an interesting candidate are *Low Data Rate* (LDR) communication systems requiring rates below $1\,\mathrm{Mbps}$ [1].

UWB-IR transmitters produce very short time domain pulses of up to $7.5\,\mathrm{GHz}$ bandwidth without the need for an additional *Radio Frequency* (RF) mixing stage due to their essentially baseband nature. This leads to significant complexity reduction at transmitter and receiver side with respect to conventional radio systems. This advantage makes UWB-IR a well suited candidate for low cost LDR applications. On the other hand, channel investigations [2] show that UWB-IR indoor channel energy is spread over a large number of multipath components. This highly increases complexity of coherent receivers as energy has to be re-combined by a large number of RAKE fingers. Furthermore, UWB-IR systems are intended to operate over a large bandwidth, overlaying bands of many other services. They are thus rigorously power constrained by regulations, as e.g., by the *Federal Communications Commission* (FCC), to minimize interference to victim receivers. These regulations impose hard performance limits to UWB-IR communication systems as energy per pulse is restricted very stringently.

In this work, we focus on UWB-IR LDR applications where a more complex *Cluster Head* (CH) communicates with many basic *Sensor Nodes* (SN). An example could be a wireless control system where only very small amount of data is transmitted from and to the SNs. At sensor side, only simple hardware structures are affordable. While the design of simple UWB-IR transmitters seems a minor problem, this is not the case for simple receivers. Only non-coherent receivers seem reasonable, which suffer from significant performance losses with respect to coherent receivers as channel energy is spread over a large number of multipath components.

Hence, we consider non-coherent *Energy Detectors* (ED) operating at very low sampling clock, i.e., below $300\,\mathrm{kHz}$, as a reasonable choice and investigate signaling schemes to efficiently increase performance of ED. The low sampling clock is applied to relax requirements on receiver sampling accuracy and to reduce power consumption.

Pulse Repetition Coding (PRC) is a known solution in asymmetric sensor networks to increase receiver performance of SNs at the expense of more transmit power at CH side. With PRC a bit is loaded on several consecutive pulses, as e.g., it is often applied in *Time-Hopping* (TH) *Pulse Position Modulation* (PPM). In LDR systems, classic PRC has two major drawbacks. First, throughput is further decreased and secondly, it does not exploit FCC power constraints efficiently.

In this paper, we present a *Modified* PRC (MPRC) coding scheme for LDR systems with receiver sampling rates of below $300\,\mathrm{kHz}$. This MPRC scheme maximizes transmit power, if FCC power constraints have to be respected. For an ED of fixed integration duration, mentioned precoding scheme is optimal, i.e., it minimizes *Bit Error Rate* (BER) by fully exploiting FCC power constraints and transmitting maximized power most efficiently. Furthermore, it is well known that performance of EDs strongly depends on the appropriate choice of the integration duration. MPRC, which requires *Channel State Information* (CSI) neither at transmitter nor at receiver side, mainly decouples receiver performance from integration duration. This has major advantages. First, performance of the ED becomes extremely robust against strong delay spread variations. Secondly, constraints on the integration duration, e.g., fixed large size due to circuit design aspects, can be compensated. Finally, jitter robustness can be increased by choosing a large integration duration. Presented MPRC, without any CSI, achieves performance of a complex *Selective* RAKE (SRAKE), at the expense of more transmit power. Presented results are based on BER performance analysis incorporating simulations using UWB channels from different measurement campaigns. Although, FCC power constraints are considered, only, results are easily adaptable to other regulations.

Applied *Modified Pulse Repetition Coded Binary Pulse Position Modulation* (MPRC-BPPM) scheme equals an orthogonal BPPM scheme of *equivalent pulses*, where each equivalent pulse consists of a sequence of equidistant copies of a basic pulse waveform, as shown in Fig. 1. The extension to dithered temporal pulse separation is straight

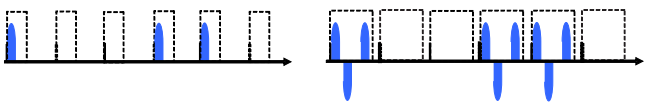

Fig. 1. Principle difference between BPPM (Left) and MPRC-BPPM (Right)

forward, but was omitted for convenience. The different copies are multiplied by an arbitrary phase in order to flatten the spectrum of the transmit signal and to minimize interference to other users, i.e., MAC.

The phases are totally ignored by the ED at the moment, but might be useful for synchronization purpose in future work. All equidistant copies of the basic waveform have the same energy E_p, which equals maximally allowed pulse energy, if a single pulse was transmitted. The pulse separation is chosen as small as possible without violating peak power constraint. Transmitter and receiver require no CSI. The transmitter is allowed to use *as much power as admitted* by the FCC, as we consider the FCC power constraints as binding enough. Due to its simplicity and great advantages, this scheme seems a very promising candidate for realization in real world LDR systems.

In the following section, the signal model is introduced and BER is analyzed. In Section III, impact of FCC power constraints on MPRC-BPPM is discussed, followed by analytic and simulation results in Section IV. In Section V, we conclude with a short summary.

II. Signal Model and BER Analysis

A. MPRC-BPPM Transmitter

The MPRC-BPPM signal sent by the transmitter is described by:

$$s_{tx}^{N_P}(t) = \sqrt{E_p} \sum_{k=-\infty}^{\infty} \sum_{n=0}^{N_P-1} \beta_i w(t - kT_f - \alpha_k \delta - n\tau_p), \qquad (1)$$

where t is the transmitter's clock time and $w(t)$ the real transmitted bandpass pulse of width T_w. The pulse is energy normalized, i.e., $\int_{-\infty}^{\infty} w^2(t)dt = 1$, and E_p is the single pulse energy. During each frame repetition time T_f, one BPPM symbol α_k is transmitted. Depending on $\alpha_k \in \{0, 1\}$, a sequence of N_P repeated pulses is either transmitted at beginning of a frame or delayed by δ. The frame repetition rate $R_f = 1/T_f$ equals the nominal BPPM pulse rate. Pulse separation $\tau_p \ll T_f$ is chosen such that peak power according to FCC power constraints is not increased with respect to single pulse transmission. To avoid *Intersymbol Interference* (ISI) between consecutive symbols and to maintain BPPM orthogonality in presence of large channel delay spread τ_c, conditions $\delta \geq (N_P - 1)\tau_p + \tau_c + T_w$ and $T_f \geq \delta + (N_P - 1)\tau_p + \tau_c + T_w$ are respected. The coefficients $\beta_i \in \{-1, 1\}$ with $i = kN_P + n$ are chosen randomly or according to a *Direct Sequence* (DS). They are applied to smooth the spectrum of the transmit signal. Thereby, transmit power can be increased, while interference to other users is kept small. In this work, the βs are ignored at receiver side. Although application of TH is straight forward, it is omitted for convenience. Especially, as very short channel occupation times of MPRC compared to classic PRC allow for other MAC schemes, as e.g., TDMA, if combined with spectral smoothing DS.

B. Energy Detector Receiver and BER Analysis

A schematic description of an ED as used in this paper can be seen in Fig. 2. The input filter $f(t)$ is assumed to be an ideal bandpass

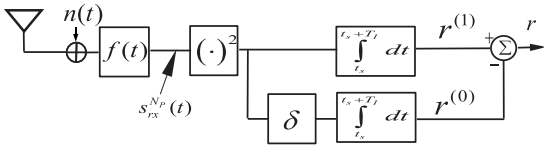

Fig. 2. Signal model of energy detector receiver

filter of bandwidth $B_{pb} \geq B$, with B the bandwidth of the transmit pulse. Hence, the receive signal is not influenced by the filter. The received signal after the bandpass filter $f(t)$ equals:

$$s_{rx}^{N_P}(t) = \sqrt{E_p} \sum_{k=-\infty}^{\infty} \sum_{n=0}^{N_P-1} \beta_i h_w (t - kT_f - \alpha_k \delta - n\tau_p) \qquad (2)$$

$$= \sqrt{E_p} \sum_{k=-\infty}^{\infty} h_{E,k} (t - kT_f - \alpha_k \delta), \qquad (3)$$

with $h_w(t)$ the convolution of the energy normalized transmit waveform and the real channel, i.e., $h_w(t) = w(t) * h(t)$. We call $h_{E,k}(t)$ the *equivalent channel*. For analysis of the uncoded BER, it is sufficient to consider only a single received frame. Therefore, we focus in the following on the k-th frame and omit index k. Assuming that $\alpha_k = 1$ was sent, the outputs of the two integrator units at time t_s are:

$$r^{(1)}(t_s) = \int_{t_s}^{t_s+T_I} \left(\sqrt{E_p} h_E(t) + \tilde{n}(t) \right)^2 dt \qquad (4)$$

$$r^{(0)}(t_s) = \int_{t_s}^{t_s+T_I} \tilde{n}^2(t - \delta) dt, \qquad (5)$$

where $\tilde{n}(t) = f(t) * n(t)$ is filtered zero-mean Additive White Gaussian Noise (AWGN) $n(t)$ with two-sided power spectral density $N_0/2$. We rewrite expression (4) as:

$$r^{(1)}(t_s) = \nu^{(1)}(t_s) + \omega^{(1)}(t_s) + \zeta^{(1)}(t_s). \qquad (6)$$

Thereby, $\nu^{(1)}(t_s) = E_p \int_{t_s}^{t_s+T_I} h_E^2(t) dt$ equals the signal energy collected by the ED and $\zeta^{(1)}(t_s) = \int_{t_s}^{t_s+T_I} \tilde{n}^2(t) dt$ is the pure (quadratic) noise term. The mixed signal-noise term is $\omega^{(1)}(t_s) = 2\sqrt{E_p} \int_{t_s}^{t_s+T_I} h_E(t) \tilde{n}(t) dt$. Due to the lack of a signal component, expression (5) simply equals:

$$r^{(0)}(t_s) = \zeta^{(0)}(t_s) \qquad (7)$$

with $\zeta^{(0)}(t_s) = \int_{t_s}^{t_s+T_I} \tilde{n}^2(t - \delta) dt$. For convenience, we omit the time t_s in the following.

Assuming *Maximum Likelihood* (ML) detection, based on the statistics of $r = r^{(1)} - r^{(0)}$, the BER conditioned on a certain channel realization $h(t)$, an integration duration T_I and a sampling instance t_s is given by:

$$P_{e|h,T_I,t_s} = P(\nu^{(1)} < \zeta^{(0)} - \zeta^{(1)} - \omega^{(1)}). \qquad (8)$$

In the following, we approximate $z = \zeta^{(0)} - \zeta^{(1)} - \omega^{(1)}$ as a Gaussian random variable. Applying quadrature sampling expansion at Nyquist rate B_{pb} [3] and central-limit theorem, we achieve:

$$\zeta^{(\alpha)} \sim \mathcal{N}\left(B_{pb} T_I N_0, B_{pb} T_I N_0^2\right), \quad \alpha \in \{0, 1\} \qquad (9)$$

for the pure quadratic noise terms and

$$\omega^{(1)} \sim \mathcal{N}\left(0, 2N_0 E_p \int_{t_s}^{t_s+T_I} h_E^2(t) dt\right) \qquad (10)$$

for the mixed signal-noise term. It can be shown that the correlation between $\omega^{(1)}$, $\zeta^{(1)}$ and $\zeta^{(0)}$ is approximately zero [4]. Hence, z can be approximated as Gaussian random variable:

$$z \sim \mathcal{N}\left(0, 2B_{pb} T_I N_0^2 + 2N_0 \nu^{(1)}\right). \qquad (11)$$

The ML performance given a certain channel realization $h(t)$, an integration duration T_I and a sampling instance t_s is now [5]:

$$P_{e|h,t_s,T_I} = \frac{1}{2} \operatorname{erfc}\left(\sqrt{\frac{(\nu^{(1)})^2}{4B_{pb} T_I N_0^2 + 4N_0 \nu^{(1)}}} \right). \qquad (12)$$

It is noteworthy that (12) strongly depends on the bandwidth of the receiver's input filter due to the term $4B_{pb} T_I N_0^2$.

III. FCC Power Constraints

A. Maximal Average and Peak Power of Antipodal Signal

A device operating under FCC's provisions of UWB indoor devices [6], has to occupy a total 10 dB bandwidth of at least 500 MHz between 3.1 and 10.6 GHz. Additionally, the emitted signal has to respect average and peak power constraint. Average power P_{av} measurements are based on spectrum analyzers with *Resolution Bandwidth* (RBW) set to $B_{av} = 1\,\text{MHz}$, RMS detector and average time window $T_{aw} = 1\,\text{ms}$. For all center frequencies f_0 of the resolution filter within 3.1 to 10.6 GHz, maximal average power $P_{av}^{\max}$ has to be below $P_{av}^{\text{FCC}} = -41.25\,\text{dBm}$. Peak power, according to [4] and [6], is best measured with a RBW of $B_p = 50$ MHz. For all center frequencies f_0 within 3.1 to 10.6 GHz, maximal peak power $P_p^{\max}$ must not exceed $P_p^{\text{FCC}} = 0\,\text{dBm}$.

According to [4], maximal average and peak power of an antipodal signal of equidistant pulses defined by $s(t) = \sqrt{E_p}\sum_{n=-\infty}^{\infty}\beta_n w(t - n/R_f)$, can be approximated very tightly as:

$$P_{av}^{\max}(R_f, f_0) = 2E_p W^2(f_0) B_{av} R_f \quad R_f \geq \tfrac{1}{T_{aw}}, \tag{13}$$

$$P_p^{\max}(R_f, f_0) = \begin{cases} \frac{2E_p W^2(f_0) B_p^2}{0.45^2} & R_f < \frac{B_p}{0.45} \\ 2E_p W^2(f_0) R_f^2 & R_f > \frac{B_p}{0.45}, \end{cases} \tag{14}$$

with $W(f)$ the Fourier transform of the pulse waveform $w(t)$. The two regimes in (14) origin from the fact that for low frame repetition frequencies resolution filtered pulses do not overlap and add up linearly in power, while for higher frequencies, they overlap and add up linear in amplitude. Next, we set the maximal powers $P_{av}^{\max}$ and $P_p^{\max}$ equal to the maximally allowed powers P_{av}^{FCC} and P_p^{FCC} and solve for $E_p W^2(f_0)$. In so doing, maximally allowed single pulse spectral energy at frequency f_0 with respect to average and peak power constraint is achieved, as shown in Fig. 3. Two different

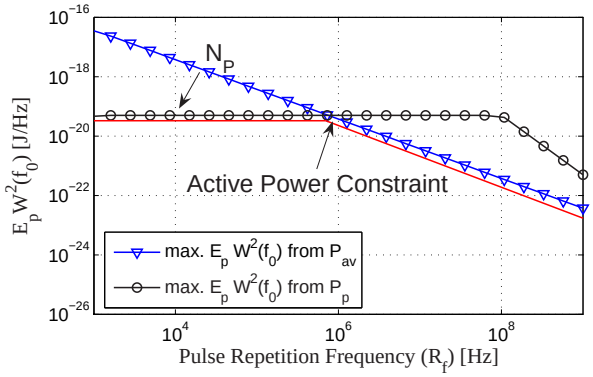

Fig. 3. Maximally allowed single pulse spectral energy

regimes can be distinguished. Peak power regime for $R_f < B_{av}$ and average power regime for $R_f \geq B_{av}$. From Fig. 3 and Eq. (14), it follows that maximal peak power does not increase for $R_f < B_p/0.45$. This is an important property we will use several times in the following section.

B. Impact of FCC Average and Peak Power Constraint on LDR MPRC-BPPM

For the rest of this paper, LDR MPRC-BPPM schemes with frame repetition rate $R_f \leq 300\,\text{kHz}$, BPPM modulation shift $\delta \leq 1/(2R_f)$, and minimal temporal pulse distance $\tau_p \geq 10\,\text{ns}$ are focused, i.e., UWB-IR operating in peak power regime. Under above system specifications, the uncoded LDR BPPM signal and the antipodal one from previous section show approximately the same maximal average and peak power, if same R_f is applied [4]. For $R_f \leq 300\,\text{kHz}$, the resolution filtered pulses are non-overlapping for both BPPM and the antipodal signal. Hence, average power is dominated by the number of pulses that fall into averaging duration $T_{aw} = 1\,\text{ms}$. As this number is the same for both, average power is approximately equal. Maximal peak power stays unchanged as minimal pulse separation is larger than $T_{\min} = 10\,\text{ns} > 0.45/B_p$. From same argumentation, it follows that MPRC-BPPM with $\tau_p \geq T_{\min} = 10\,\text{ns}$ shows the same peak power as corresponding antipodal signal. For maximal MPRC-BPPM average power, an accurate upper bound can be found assuming that each doubling of MPRC pulses increases BPPM average power by 6 dB. This assumption is equivalent to assuming average power resolution filtered pulses as totally overlapping and therefore, adding up perfectly in amplitude. As average power filtered pulses extend over about 2μs and due to MPRC are separated by only a few nanoseconds, this is a reasonable assumption. Hence, maximal average and peak power for LDR MPRC-BPPM of N_P pulses equals:

$$P_{av}^{\max}(R_f, f_0) = 2E_p W^2(f_0) B_{av} N_P^2 R_f \tag{15}$$

$$P_p^{\max}(R_f, f_0) = \frac{2E_p W^2(f_0) B_p^2}{0.45^2} \tag{16}$$

and the maximally allowed single pulse spectral energy:

$$E_{p,av}^{\text{MPRC}} W^2(f_0) = \frac{P_{av}^{\text{FCC}}}{2N_P^2 R_f B_{av}} \tag{17}$$

$$E_{p,p}^{\text{MPRC}} W^2(f_0) = \frac{0.45^2 P_p^{\text{FCC}}}{2B_p^2}. \tag{18}$$

According to Fig. 3, FCC power constraints are fully exploited, if maximally allowed single pulse spectral energies in (17) and (18) are equal, i.e., if average power is increased to its maximally allowed value, while keeping peak power constant. By equating the two expressions and solving for N_P, maximal number of precoding pulses is found which can be applied without violating FCC power constraints [7]:

$$N_P^{\max} = \left\lfloor \sqrt{\frac{1}{0.45^2 R_f} \frac{B_p^2}{B_{av}} \frac{P_{av}^{\text{FCC}}}{P_p^{\text{FCC}}}} \right\rfloor, \tag{19}$$

It is remarkable that (19) scales with $1/\sqrt{R_f}$, which is due to the fact that average power in (13) for $R_f \leq 1\,\text{MHz}$ scales with R_f. Examples of (19) are: 2 pulses at 200 kHz, 3 at 100 kHz and 6 at 20 kHz. The number of MPRC pulses that can be applied is quite restricted, all the same significant performance improvement is possible.

IV. Results

A. Normalization

For the BER curves presented, we apply an unusual *Signal-to-Noise Ratio* (SNR) normalization. We normalize the SNR to the total received energy, if a single pulse of 500 MHz bandwidth is transmitted in the band from 3.1 to 3.6 GHz. Hence, SNR is defined as:

$$\xi = \frac{E_{h,500}}{N_0} = \frac{E_{p,500}}{N_0} \int_{-\infty}^{\infty} \left(\int_{-\infty}^{\infty} w_{500}(\tau) h(t-\tau) d\tau \right)^2 dt \tag{20}$$

with $w_{500}(t)$ the normalized pulse shape and $E_{p,500}$ the energy of the transmit pulse of 10 dB bandwidth 500 MHz. Note that a 500 MHz pulse has approximate energy $E_{p,500} \approx BE_0$, while a pulse of 7.5 GHz bandwidth has approximately 15 times more. Hence, we do not normalize SNR to the total received energy, as it would be necessary to show BER curves as a function of receive SNR.

Justification is that in UWB-IR radiated power is not the dominant factor in system power consumption but is rigorously limited by power constraints[1]. With this normalization, additional receive power due to increased number of MPRC pulses as well as increased bandwidth appears as BER improvements. The conditional BER is now:

$$P_{e|h,t_s,T_I} = \frac{1}{2}\operatorname{erfc}\left(\frac{\xi\frac{\nu^{(1)}}{E_{h,500}}}{\sqrt{4B_{pb}T_I + 4\xi\frac{\nu^{(1)}}{E_{h,500}}}}\right). \quad (21)$$

B. Optimal Temporal Pulse Separation for MPRC

In this Section, it is shown for fixed integration duration T_I that a pulse separation of $\tau_p = T_{\min}$ is optimal. From (21), it is evident that for fixed T_I, BER depends only on instantaneous SNR or more precisely, on $x = \left(\xi\frac{\nu^{(1)}}{E_{h,500}}\right)$. Although, evaluation of the exact pairwise error probability is straight forward [8], average SNR investigations are considered as meaningful enough, i.e., $\mathcal{E}\{P(e|h(t))\}$ is approximated by $P\left(e|\mathcal{E}\left\{h^2(t)\right\}\right)$ with $\mathcal{E}\{\cdot\}$ the expectation operator. This approximation is close, if instantaneous SNR shows little variation over a small area. Due to the high multipath resolution inherent in UWB *Channel Impulse Responses* (CIR), this is a reasonable assumption. For $x > 0$, the expression within the brackets of (21) is a monotonic growing function of x. Hence, average receive energy $\mathcal{E}\left\{\nu^{(1)}\right\}$ shall be maximized by optimization of MPRC pulse separation τ_p, if FCC power constraints are considered. While maximally allowed number of MPRC pulses is limited by the average power constraint, optimal pulse separation is determined by the peak power constraint. Taking into account FCC peak power constraint and assuming, that maximally allowed power is radiated by the transmitter, captured signal energy per frame can be described as:

$$\begin{aligned}\mathcal{E}\left\{\nu^{(1)}\right\} &= \frac{\operatorname{argmax}_{t,f_0}\left\{|w(t)*g_{f_0}(t)|^2\right\}}{\operatorname{argmax}_{t,f_0}\left\{\left|\sum_{n=0}^{N_P-1}\beta_n w(t-n\tau_p)*g_{f_0}(t)\right|^2\right\}} \\ &\quad \cdot E_p\mathcal{E}\left\{\int_{t_s}^{t_s+T_I}\left(\sum_{n=0}^{N_P-1}\beta_n h_w(t-n\tau_p)dt\right)^2\right\} \quad (22)\\ &= K_c E_p \mathcal{E}\left\{\int_{t_s}^{t_s+T_I} h_E^2(t)dt\right\}. \quad (23)\end{aligned}$$

The second line of (22) equals signal energy collected by the ED, if all N_P pulses are transmitted with maximally allowed single pulse energy. Doing so is allowed for $\tau_p \geq T_{\min}$, only. $K_c \leq 1$ describes the correction factor by which transmit pulse energy has to be reduced, if τ_p is chosen smaller than $T_{\min}$. According to the FCC [4], [6], bandwidth of the spectrum analyzer's sweeping filter $g_{f_0}(t)$ is set to 50 MHz. Center frequency f_0 is swept from 3.1 to 10.6 GHz.

In detail, K_c describes the ratio between maximal single pulse and maximal MPRC peak power. It equals 1 for $\tau_p \geq T_{\min}$ and is smaller than 1 for $\tau_p < T_{\min}$. By assuming the spectral energy of the transmit pulse $w(t)$, i.e., $|W(f)|^2$, to be constant over its supported band, K_c can be approximated by:

$$K_c \approx \tilde{K}_c = \frac{1}{\operatorname{argmax}_t\left\{\left|\sum_{n=0}^{N_P-1}\tilde{g}(t-n\tau_p)\right|^2\right\}}, \quad (24)$$

with $\tilde{g}(t)$ a sweeping filter of center frequency $f_0 = 0$ and peak amplitude 1. From FCC power constraint discussion, it is evident that the coefficients β_n have little impact on K_c [4], and are therefore omitted. As a typical example for $\tilde{g}(t)$, we take a Gaussian filter, which is often used in spectrum analyzers. As a typical CIR, we consider a *Gaussian Random Process* (GRP) with exponentially decaying *Average Power Delay Profile* (APDP):

$$h_w(t) = \hat{e}^{-\frac{\gamma}{2}t}v(t), \quad (25)$$

where $v(t)$ is a zero-mean white GRP of two-sided power spectral density 1, filtered by an ideal bandpass filter of bandwidth B, i.e., $\sigma_v^2 = 2B$, γ is a decay coefficient and

$$\hat{e}^{-x} = \begin{cases} e^{-x} & \text{if } x \geq 0 \\ 0 & \text{else} \end{cases}. \quad (26)$$

As $B \gg \frac{1}{\gamma}$, the energy collected by the ED can be approximated as [4]:

$$E_p\mathcal{E}\left\{\int_{t_s}^{t_s+T_I} h_w^2(t)dt\right\} \approx 2BE_p\int_{t_s}^{t_s+T_I}\hat{e}^{-\gamma t}dt \quad (27)$$

for single pulse transmission. For MPRC, we achieve:

$$\mathcal{E}\left\{\nu^{(1)}\right\} \approx 2BE_p\tilde{K}_c\int_{t_s}^{t_s+T_I}\sum_{n=0}^{N_P-1}\hat{e}^{-\gamma(t-n\tau_p)}dt = \tilde{K}_c E_{\text{MPRC}} \quad (28)$$

with E_{MPRC} the energy that an ED would collect if no peak power had to be respected, i.e., if $E_{tx} = N_P E_p$.

To achieve more intuition into the behavior of (28) and its impact, we consider two different scenarios and upper bound E_{MPRC} by the energy $E_{\text{MPRC}}^{(u)}$, that would be collected if $h_w(t)$ had uniform APDP, i.e., $\gamma = 0$. We define N_{fit} as the maximal number of pulses that fit into an integration duration T_I, i.e., $N_{\text{fit}} = \lfloor T_I/\tau_p \rfloor$.

Scenario 1: We consider both integration time T_I and number of MPRC pulses $N_P \leq N_{\text{fit}}$ as fixed. Then $E_{\text{MPRC}}^{(u)}$ increases linearly as a function of $\Delta\tau_p$:

$$\Delta E_{\text{MPRC}}^{(u)}(\Delta\tau_p) = \sum_{n=0}^{N_P-1} n\Delta\tau_p = \frac{N_P(N_P-1)}{2}\Delta\tau_p, \quad (29)$$

where new pulse separation equals $\tau_p^{\text{new}} = \tau_p^{\text{old}} - \Delta\tau_p$. Due to $E_{\text{MPRC}}^{(u)} \geq E_{\text{MPRC}}$, it is evident that E_{MPRC} increases at most linearly with decreasing τ_p. On the other hand, (24) stays constant for $\tau_p \geq T_{\min}$ and decreases quadratically with decreasing $\tau_p < T_{\min}$. Hence, $\tau_p = T_{\min}$ is the best choice.

Scenario 2: We assume that the transmitter always sends N_{fit} pulses. Then, we can formulate an upper found for $E_{\text{MPRC}}^{(u)}$:

$$E_{\text{MPRC}}^{(u)}(\tau_p) \leq \sum_{n=0}^{N_{\text{fit}}} n\tau_p = \frac{N_{\text{fit}}(N_{\text{fit}}+1)}{2}\tau_p \approx \frac{T_I^2}{2\tau_p} + \frac{T_I}{2}. \quad (30)$$

It is evident that $E_{\text{MPRC}}^{(u)}(\tau_p)$ grows faster now. All the same, by inspection of (24) and (30) for reasonable values, it becomes evident that $\tilde{K}_c$ still decreases faster than $E_{\text{MPRC}}^{(u)}(\tau_p)$ increases, for $\tau_p < T_{\min}$. Hence, in this scenario, $\tau_p = T_{\min}$ is the best choice for MPRC, too.

In Fig. 4, $1/\tilde{K}_c$ is plotted for N_{fit} MPRC pulses, where N_{fit} depends on τ_p. The correction factor $\tilde{K}_c$, which does not depend on γ, decreases drastically for $\tau_p < T_{\min}$. Compared to FCC or NTIA [9] evaluations, the minimal pulse separation seems too restrictive. In Fig. 4, it is $T_{\min} \approx 15\,\text{ns}$, while evaluation from FCC power constraint shows $T_{\min} = 10\,\text{ns}$. This is due to the assumptions made in (24). All the same, the impact of power constraints is shown very clearly. In Fig. 5, E_{MPRC} gains with respect to E_{MPRC} at $\tau_p = 50\,\text{ns}$ are shown for different exponentially decaying channels defined by

[1]Plotting BER over receive SNR cancels out gains due to higher transmit power.

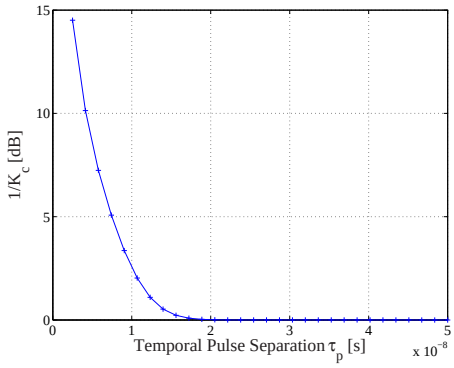

Fig. 4. Inverse correction factor $1/\tilde{K}_c$

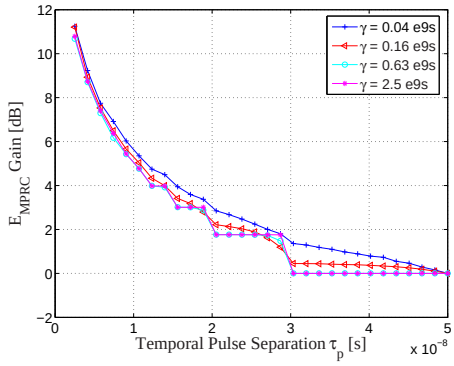

Fig. 5. E_{MPRC} gain due to decreasing τ_p

(25). The integration duration of the ED was fixed to $T_I = 60\,\text{ns}$. The plots confirm our result, that for decreasing $\tau_p < T_{\text{min}}$, $1/K_c$ grows much faster than E_{MPRC}. In Fig. 6, the BERs are plotted as a function of τ_p for $\text{SNR} = 15\,\text{dB}$. The optimum $\tau_p = T_{\text{min}}$ can be nicely identified. These BER curves have been obtained without the need of approximations and approve the reasonability of our approximations used for above discussion. The error floors for $\gamma = 2.5 \cdot 10^9\,\text{s}$ and $\gamma = 6.3 \cdot 10^8\,\text{s}$ origin from the fact that the corresponding CIR have very small delay spread and are non-overlapping for $\tau_p \geq 20\,\text{ns}$. Then significant BER changes occur, only, if the number of pulses within the integration window decreases. Hence, the high degradations at $\tau_p = 20\,\text{ns}$ and $\tau_p = 30\,\text{ns}$ occur because energy of an overall CIR output slips out of the integration window. BER curves for small γs are significantly worse than for larger ones as a higher percentage of total channel output energy falls out of the integration window for smaller γs.

Summarizing results, we argue in the following that MPRC-BPPM with $\tau_p = T_{\text{min}}$ is optimal for EDs of fixed integration duration T_I. First, recall that for fixed T_I only the amount of energy concentrated

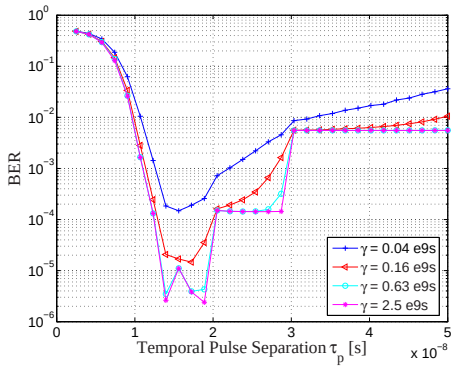

Fig. 6. BER of ED for different τ_p and γ at $\text{SNR} = 15\,\text{dB}$

in T_I influences the BER and that the specific shape of the receive signal is irrelevant. From *Scenario 2*, we know that for $N_P^{\max} \geq N_{\text{fit}}$, $\tau_p = T_{\text{min}}$ is optimal. Whether $N_P^{\max} \geq N_{\text{fit}}$ is satisfied or not depends on the frame repetition rate. For fixed $N_P^{\max} < N_{\text{fit}}$, we have shown that $\tau_p = T_{\text{min}}$ is optimal, as well. Furthermore, as the BER of EDs depends only on the amount of energy in fixed T_I, it is evident that pulsing with $N_P > N_P^{\max}$ decreases performance with respect to $N_P = N_P^{\max}$ as energy per pulse has to be reduced to comply with average power constraint. Hence, we have following result:
For EDs of fixed integration duration T_I, MPRC-BPPM with pulse separation $\tau_p = T_{\text{min}}$ and number of MPRC pulses:

$$N_P \quad = \quad \begin{cases} N_{\text{fit}} & \text{for} \quad N_P^{\max} \geq N_{\text{fit}} \\ N_P^{\max} & \text{for} \quad N_P^{\max} < N_{\text{fit}} \end{cases} \tag{31}$$

is optimal.

C. Simulation Results

BER performance results for LDR MPRC-BPPM systems are presented based on different measured UWB CIRs with bandwidth B from $500\,\text{MHz}$ up to $7.5\,\text{GHz}$. They are obtained by evaluating the captured energy $\nu^{(1)} = E_p \int_{t_s}^{t_s+T_I} h_E^2(t)dt$, plugging it into (21) and averaging at least over 100 CIRs. Transmit pulse is a Gaussian bandpass pulse.

Most of used UWB channels are taken from a UWB measurement campaign performed at ETHZ [7], [10] in a SPIN (Sensor, Positioning and Identification Network) or warehouse like scenario, i.e., in a rich scattering environment similar to [11]. The equipment is restricted to a frequency range of 3 to $6\,\text{GHz}$. A total of 4500 CIRs in 22 different LOS and NLOS areas has been measured.

In order to demonstrate MPRC-BPPM over channels extending over the entire UWB bandwidth, we simulate also using channels taken from a measurement campaign at IMST [12]. These measurements were performed with a network analyzer of frequency range 1 to $11\,\text{GHz}$ in an office building and were among others basis for well-known IEEE 802.15a UWB channel model.
The LDR MPRC-BPPM scheme considered has frame repetition rate $R_f \leq 300\,\text{kHz}$, BPPM modulation shift $\delta \leq 1/(2R_f)$ and $\tau_p \geq T_{\text{min}} = 10\,\text{ns}$.

In Fig. 7 and Fig. 8, MPRC-BPPM in conjunction with an ED is compared to single pulse transmission combined with a coherent *Selective RAKE* (SRAKE) of 20 fingers. This number of fingers was chosen as a reasonable upper limit for realistic RAKE receivers. Simulations are performed with a transmit pulse of $2.9\,\text{GHz}$ bandwidth using NLOS channels from ETHZ. In Fig. 7, the SRAKE is compared to an ED applying integration duration which is optimally adjusted to the channel. As expected, the ED suffers from significant performance losses with respect to the SRAKE, i.e., about $5\,\text{dB}$ in SNR at $\text{BER} = 10^{-3}$. But the ED combined with MPRC-BPPM of only $N_P = 3$ pulses outperforms the SRAKE in conjunction with single pulse transmission. Thus, MPRC-BPPM without any CSI performs better than the very complex SRAKE, at the expense of more transmit power. As perfect window adjustment is still involved, we compare an ED of fixed large integration duration $T_I = 200\,\text{ns}$, in Fig. 8. Confirming intuition, the ED of fixed T_I performs even worse than the optimal one. It is remarkable though that combined with MPRC-BPPM, it strongly improves its performance and for $N_P = 4$ outperforms the SRAKE at high SNR. In Fig. 9, SNR at $\text{BER} = 10^{-3}$ is shown as a function of number of MPRC pulses N_P and pulse bandwidth B. It is important to note that the transmit energy within one frame, scales with both B and N_P according to (21), i.e., $E_{tx} \approx N_P B E_0$. The channels used for this simulation, are

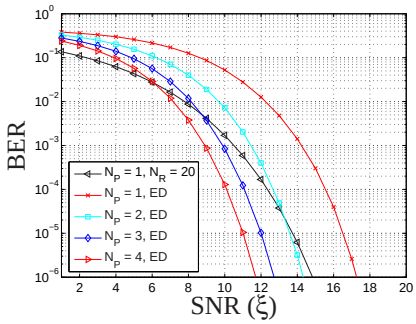

Fig. 7. BER comparison between ED of optimal (adjusted) integration duration and 20 finger SRAKE.

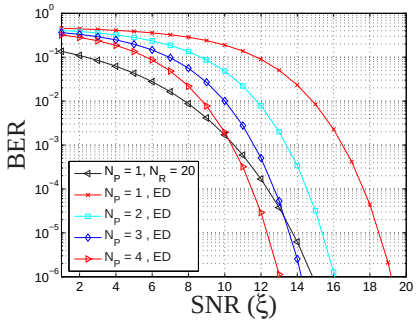

Fig. 8. BER comparison between ED of fixed integration duration and 20 finger SRAKE.

taken from NLOS measurements performed at IMST. While there are major performance gains, if the number of transmitted MPRC pulses is increased, there are hardly any gains, if bandwidth is increased. E.g., if $N_P = 3$ MPRC pulses of $B = 500$ MHz are transmitted, SNR performance of the ED at BER $= 10^{-3}$ increases by 5 dB with respect to a single transmit pulse of 500 MHz bandwidth. This is achieved at the expense of three times more power. But if three times more power is radiated by increasing bandwidth of the transmit pulse to 1.5 GHz, there is at most a gain of 2 dB in SNR. This phenomenon mainly occurs due to frequency dependent pathloss effects. While noise power at the receiver, increases linearly with B, this is not the case for the received signal power, due to stronger pathloss at higher frequencies. Hence, as shown in [5], there exists an optimal bandwidth. Although broader bandwidth increases diversity gains, with respect to BER, one might prefer spending energy in additional MPRC pulses, if $N_P < N_P^{\max}$ is satisfied, prior to increasing pulse bandwidth. Further advantages of MPRC-BPPM

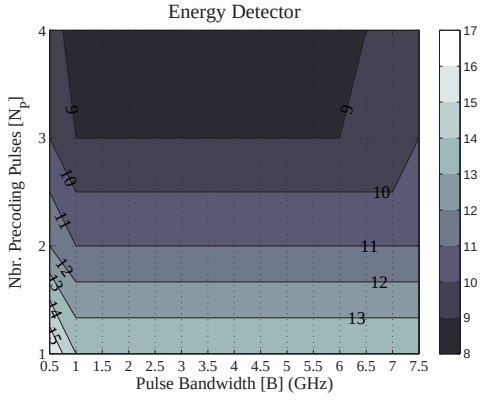

Fig. 9. SNR in dB at BER $= 10^{-3}$ plotted as a function of N_P and B.

are that with increasing number of MPRC pulses, BER performance of the ED of fixed integration duration becomes more and more robust against delay spread variations of the channel. This is because MPRC artificially increases delay spread such that the importance of the real channel delay spread is significantly reduced. Hence, outage probability can be drastically reduced. This has the major advantage, that involved integration duration adaption can be omitted. Furthermore, if hardware constraints do not allow realization of integrators with extreme short T_I, MPRC is a helpful approach to compensate for possibly too large integration windows. It is evident that MPRC also increases jitter robustness and that it helps to significantly relax synchronization requirements.

V. Conclusions

We have presented a simple modified pulse repetition coding scheme, that fully exploits FCC power constraints and significantly improves performance of EDs in LDR systems. It has been demonstrated that for fixed integration duration T_I, MPRC-BPPM is optimal. MPRC-BPPM was shown to outperform the SRAKE at expense of more transmit power. It was discussed that it is preferable to distribute power over several MPRC pulses than over huge bandwidth and that MPRC-BPPM can be used to make ED performance almost independent of the adequate integration window. This makes EDs robust against delay spread variations and reduces hardware requirements.

VI. Acknowledgement

The authors would like to thank all partners of the PULSERS project (www.pulsers.net), that is partially funded by the European Commission and the Swiss Federal Office for Education and Science, for their contributions and constructive discussions.

References

[1] I. Oppermann, L. Stoica, A. Rabbachin, Z. Shelby, and J. Haapola, "UWB wireless sensor networks: UWEN - a practical example," *IEEE Commun. Mag.*, vol. 42, pp. 27–32, Dec. 2004.

[2] J. Foerster, "Channel modeling sub-committee report final," IEEE P802.15 02/490r1–SG3a, Tech. Rep., Feb. 7, 2003.

[3] R. G. Vaughan, N. L. Scott, and W. D. Rod, "The theory of bandpass sampling," *IEEE Trans. Signal Processing*, vol. 39, no. 9, Sept. 1991.

[4] M. Weisenhorn and W. Hirt, "Impact of the FCC average- and peak power constraint on the power of UWB radio signals," In PULSERS, Tech. Rep. D3b4b-Annexe, Apr. 2004.

[5] ——, "Robust noncoherent receiver exploiting UWB channel properties," in *Joint UWBST & IWUWBS*, Kyoto, Japan, May 18–21, 2004, pp. 156–160.

[6] FCC, "Revision of part 15 of the commission's rules regarding ultra-wideband transmission systems," *First Report and Order, ET-Docket 98-153, FCC 02-28*, adopted/released Feb. 23, 2004/Apr. 22, 2002.

[7] F. Troesch, F. Althaus, and A. Wittneben, "Pulse position pre-coding exploiting UWB power constraints," in *Proc. SPAWC*, New York, NY, Jun. 5–8, 2005.

[8] D. Tse and P. Viswanath, *Fundamentals of Wireless Communication*. Cambridge University Press, Sept. 2004.

[9] J. P. C. Roosa, "Assessment of compatibility between ultrawideband devices and selected federal systems," NTIA, Tech. Rep. 01–43, Jan. 2001.

[10] F. Althaus, F. Troesch, T. Zasowski, and A. Wittneben, "Spatio-temporal signature measurement and characterization," In PULSERS, Tech. Rep. D3b6a, Dec. 2004.

[11] J. Karedal, S. Wyne, P. Almers, F. Tufvesson, and A. Molisch, "UWB channel measurements in an industrial environment," in *IEEE Proc. GLOBECOM*, vol. 6, no. 29, Dallas, TX, Nov. 29 – Dec. 3, 2004, pp. 3511–3516.

[12] J. Kunisch and J. Pamp, "Measurement results and modeling aspects for the UWB radio channel," in *IEEE Conf. on UWB Sys. and Tech. (UWBST)*, Baltimore, MD, May 21–23, 2002, pp. 19–23.